Royal Netherlands Meteorological Institute
Ministry of Infrastructure and Water Management

ISTITUTO NAZIONALE DI GEOFISICA E VULCANOLOGIA

A method to correct superconducting gravity recordings for the effect of rainfall and snow melting applied to Mt. Etna volcano, Italy

Mathijs R. Koymans [1,2], Flavio Cannavò [3], and Daniele Carbone [3], Elske de Zeeuw-van Dalfsen [1,2] Contact: mathijs.koymans@knmi.nl

Continuous gravimetry observations encompass many geophysical phenomena of varying amplitudes and periods. In the framework of NEWTON-g, continuous gravimetry will be used to monitor mass changes in the subsurface surrounding Mt. Etna, Sicily, Italy. The transient gravity signature of local precipitation and snow melting may obscure volcano-related gravity observations. We present a method to correct for the effect of shallow hydrological processes using rain gauge data, GNSS-IR for snow melt estimates, and a hydrological transfer function that converts precipitation and snow melt to an expected relative gravity change.

Introduction

We study the transient effect of groundwater mass changes on the observed gravity signal from a superconducting gravimeter deployed on Mt. Etna, Italy. Gravimeters are capable of detecting minor changes in the vertical component of gravity over time scales from minutes to years. Insight on geophysical phenomena that cause mass displacements in the subsurface can thus be obtained through the use of gravimetry that may otherwise remain concealed. Gravity recordings contain multiple components which contribute to the signal with different magnitudes, such as earth tides, atmospheric pressure, and local hydrology. These components need to be precisely evaluated, in order to isolate a possible volcanic signal. Here, we study the effect of groundwater mass changes on gravity, as a result of rainfall and snow melting, the latter estimated through GNSS interferometric reflectometry. A forward charge-discharge model is used to compare gravity recordings between 2018 - 2019 with observed and esimated precipitation events. We show that the observed gravity signal cannot be explained only through changes in groundwater mass, implying that other, possibly volcanic processes must have been at play.

Figure 1: Geographical location showing site Serra La Nave (alt: 1735 m) where the superconducting gravimeter is deployed on Mt. Etna, Sicily, Italy. Source: Google Maps.

Precipitation Data

To model the subsurface response to precipitation events, good control on solid (snow) and wet (rain) precipitation is required. Rain measurements are available from a weather station that is co-located with the superconducting gravimeter. Direct measurements of snow height are absent and must be estimated.

Snow Depth Estimates

Local snow depth is estimated through a GNSS receiver, using the technique of GNSS Interferometric Reflectometry (GNSS-IR) developed by Larson & Nievinski (2012). Constructive and deconstructive interference between direct and reflected multipath waves from GNSS satellites impose changes in the relative signal amplitudes that are correlated with the distance from the antenna to a reflective ground surface, and thus inversely proportional to snow depth. The signal-to-noise (SNR) ratio of the recorded signal is proportional to:

$$\mathrm{SNR} \propto \cos\left(4\pi h \lambda^{-1} \sin\theta\right) \qquad (1)$$

Where λ represents the wavelength of the GNSS L1 ($\sim$ 19.03 cm) or L2 ($\sim$ 4.42 cm) carrier frequencies. The angle θ represents the observed satellite elevation in rad, h the distance to the reflective surface in m. This equation represents that of a simple harmonic motion of the form: $A \cos \omega t$, where the reflector height term h is included in the angular frequency ω. This dominant frequency can be recovered through a spectral analysis (Lomb-Scargle periodogram; Fig. 3) of the SNR as a function of the sine of the observed satellite elevation angle θ as shown in Fig. 2, and thus converted to reflector height following Eq. 1.

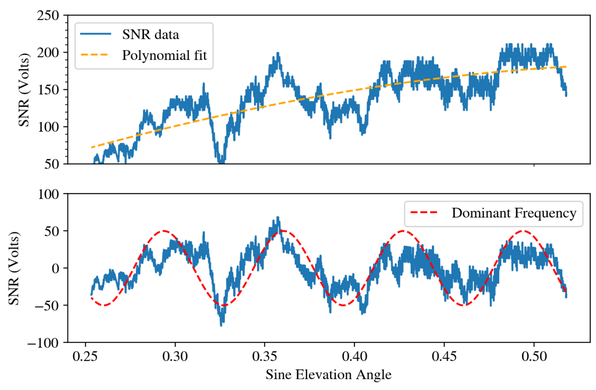

*Figure 2: The relationship between the SNR (Volts) and the sine of the apparent elevation angle of the satellite (blue). **Top**) a second order polynomial detrend is applied (orange) to eliminate long period leakage, and **bottom**) the dominant angular frequency is recovered (red) through the periodogram in Fig. 3.*

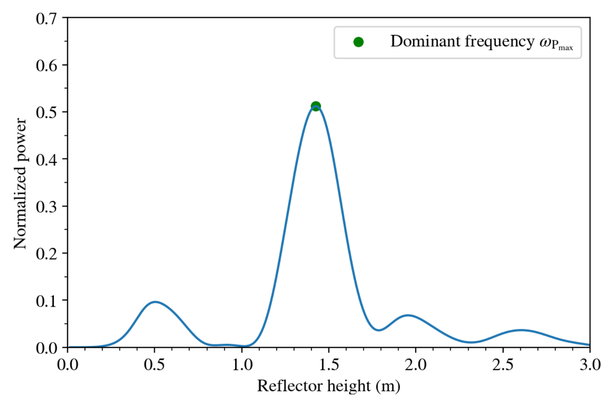

Figure 3: Lomb-Scargle periodogram of the data in Fig. 2. The dominant frequency ω is converted to a reflector height following Eq. 1.

Figs. 2 and 3 show the process for a single satellite overhead pass, while a total of 32 GPS satellites are available. We obtain the best results for reflections from a certain azimuthal range, depending on the quality of the reflection track, which varies due to terrain, vegetation, or canopies breaking the satellite line-of-sigth. Fig. 4 shows estimated reflector height for three satellites as function of date, colored by satellite azimuth. Lower azimuths (between 20 and 70 degrees) give stable reflector heights, while reflections from higher azimuths are increasingly scattered.

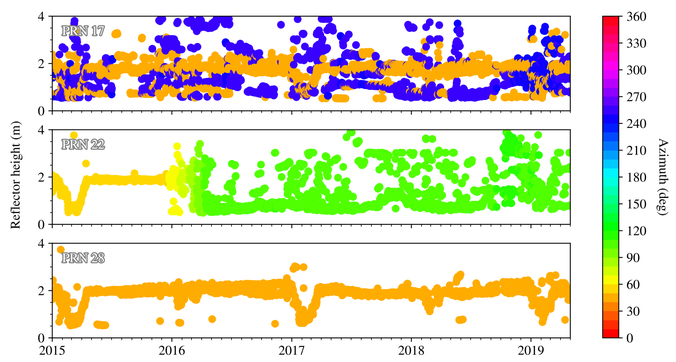

Figure 4: Estimated reflector heights for three satellites with PRN identifiers 17, 22, and 28 as a function of time and reflection azimuth.

The calculation is repeated for all reflections within the acceptable azimuth range $20 < \phi < 70$ and plotted in Figure 5. A running median is used to smooth the result, and reflector heights are then inverted to local snow depth. The negative gradient of snow depth is assumed to the amount of meltwater contributing to the groundwater balance.

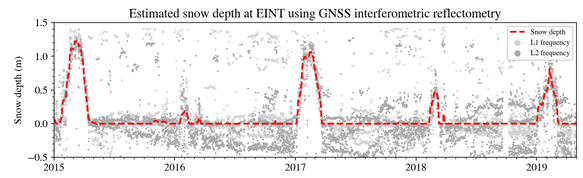

Figure 5: Estimated snow depths using GNSS-IR between 2015 - 2019 at site Serra La Nave, Sicily. Clear peaks can be identified in winter with a maximum snow cover of 1.2 m.

Relating Precipitation to Gravity

We apply the forward groundwater model derived by Crossley (1998) that uses an exponential fast charge ($\tau_1 = 21$d) and slow discharge ($\tau_2 = 258$d) model (Eq. 2), illustrated by the green curve in Fig. 6. A scaling factor of $K_{hg} = 38\,\mu$Gal/m and snow density factor $K_{sw} = 0.34$ are used to relate the mass of rain and snow melt to gravity change. The model parameters were previously fitted to gravity data between 2015 - 2017 at the same site. The model suggests that rainwater moves beneath the gravimeter at a fast rate, and slowly infiltrates deeper into the soil until the gravimeter is no longer sensitive enough.

$$g(t) = \sum_{x=t_0}^{t} K_{hg}\left(K_{sw}\delta_{x(snow)} + \delta_{x(rain)}\right)\left(1 - e^{-\frac{t-x}{\tau_1}}\right)\left(e^{-\frac{t-x}{\tau_2}}\right) \qquad (2)$$

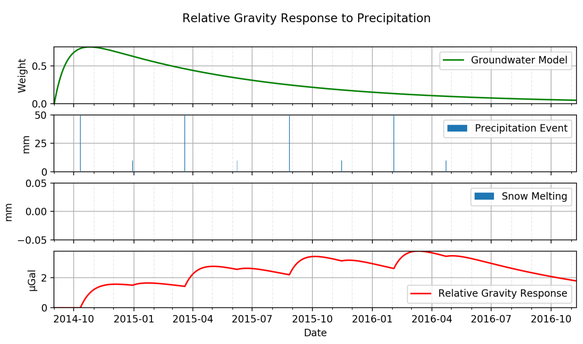

Figure 6: Example model by convolving the exponential charge-discharge function (green) and daily precipitation impulses (blue) to calculate the expected gravity signal through time (red). No snow melting is assumed.

The final results including measured precipitation data and snow melt estimates are shown in Figure 7, and compared to the observed superconducting gravimeter data. There is a good alignment with the gravity data, except for the sudden drop and recovery in gravity around the start of 2019 that cannot be explained by local precipitation or meltwater.

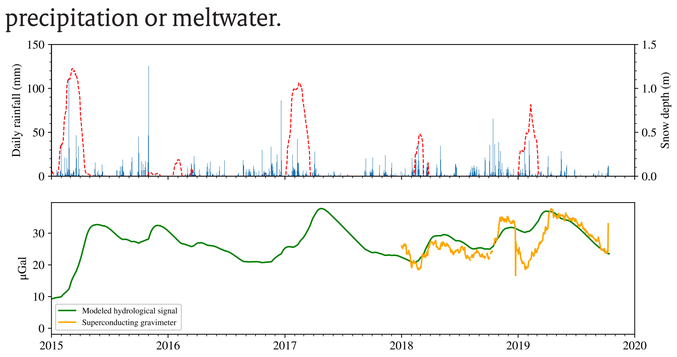

Figure 7: The final results including measured precipitation (blue) snow depth estimates (red), are shown in Fig. 7. The modelled gravity signal (green) compared to the observed signal by the superconducting gravimeter (orange).

Conclusion

We show that through the combined efforts of GNSS-IR and a simple forward hydrological model we can estimate the gravity response of precipitation and deduct it from the observations. We succefully identify a gravity signal unrelated to local hydrology that must be induced by another (volcanic) processes and should be further investigated.

[1] R&D Department of Seismology and Acoustics, Royal Netherlands Meteorological Institute. PO Box 201, 3730 AE De Bilt, The Netherlands. [2] Geoscience and Engineering, Delft University of Technology. [3] Istituto Nazionale di Geofisica e Vulcanologia, Sezione di Catania, Osservatorio Etneo, Catania, Italy

Crossley, D. (1997). Comprehensive analysis of 2 years of sg data from table mountaincolorado. InProc. 13th int. symp. on earth tides
Larson, K. M.,& Nievinski, F. G. (2012). GPS snow sensing: results from the EarthScope plate boundary observatory. GPS Solutions, 17(1), 41-52